Engineering Geology 168 (2014) 120–128

Contents lists available at ScienceDirect

Engineering Geology

journal homepage: www.elsevier.com/locate/enggeo

Slope reliability analysis considering spatially variable shear strength parameters using a non-intrusive stochastic finite element method

Shui-Hua Jiang [a], Dian-Qing Li [a,*], Li-Min Zhang [b], Chuang-Bing Zhou [a]

[a] State Key Laboratory of Water Resources and Hydropower Engineering Science, Key Laboratory of Rock Mechanics in Hydraulic Structural Engineering (Ministry of Education), Wuhan University, 8 Donghu South Road, Wuhan 430072, PR China
[b] Department of Civil and Environmental Engineering, The Hong Kong University of Science and Technology, Clear Water Bay, Kowloon, Hong Kong

ARTICLE INFO

Article history:
Received 31 July 2013
Received in revised form 31 October 2013
Accepted 10 November 2013
Available online 16 November 2013

Keywords:
Slopes
Shear strength
Spatial variability
Random field
Reliability
Stochastic finite element method

ABSTRACT

This paper proposes a non-intrusive stochastic finite element method for slope reliability analysis considering spatially variable shear strength parameters. The two-dimensional spatial variation in the shear strength parameters is modeled by cross-correlated non-Gaussian random fields, which are discretized by the Karhunen–Loève expansion. The procedure for a non-intrusive stochastic finite element method is presented. Two illustrative examples are investigated to demonstrate the capacity and validity of the proposed method. The proposed non-intrusive stochastic finite element method does not require the user to modify existing deterministic finite element codes, which provides a practical tool for analyzing slope reliability problems that require complex finite element analysis. It can also produce satisfactory results for low failure risk corresponding to most practical cases. The non-intrusive stochastic finite element method can efficiently evaluate the slope reliability considering spatially variable shear strength parameters, which is much more efficient than the Latin hypercube sampling (LHS) method. Ignoring spatial variability of shear strength parameters will result in unconservative estimates of the probability of slope failure if the coefficients of variation of the shear strength parameters exceed a critical value or the factor of slope safety is relatively low. The critical coefficient of variation of shear strength parameters increases with the factor of slope safety.

1. Introduction

In recent years, the spatial variability of soil properties has received considerable attention in slope stability analysis. Many investigators have contributed to this subject (e.g., Griffiths and Fenton, 2004; Cho, 2007; Low et al., 2007; Srivastava and Sivakumar Babu, 2009; Cho, 2010; Srivastava et al., 2010; Griffiths et al., 2011; Wang et al., 2011; Cho, 2012; Ji et al., 2012; Li et al., 2013c; Zhu and Zhang, 2013). For example, Griffiths and Fenton (2004) studied the effect of spatial variability of undrained shear strength on the probability of slope failure using random finite element method. Cho (2007) investigated the effect of spatially variable soil properties on the slope stability using direct Monte Carlo simulations (MCS). Low et al. (2007) proposed a practical EXCEL procedure to analyze slope reliability in the presence of spatially varying shear strength parameters. Srivastava and Sivakumar Babu (2009) quantified the spatial variability of soil parameters using field test data and evaluated the reliability of a spatially varying cohesive–frictional soil slope. Cho (2010) investigated the effect of spatial variability of shear strength parameters accounting for the correlation between cohesion and friction angle on the slope reliability. Srivastava et al. (2010) investigated the effect of spatial variability of permeability parameter on steady state seepage flow and slope stability. Griffiths et al. (2011) performed a probabilistic analysis to explore the influence of spatial variation in the shear strength parameters on the reliability of infinite slopes. Wang et al. (2011) developed a subset simulation-based reliability approach for slope stability analysis considering spatially variable undrained shear strength. Ji et al. (2012) adopted the First Order Reliability Method (FORM) coupled with a deterministic slope stability analysis to search the critical slip surface when the spatial variability in the shear strength parameters is considered.

In the majority of these studies, the traditional limit equilibrium method (LEM) is used to perform deterministic slope stability analyses. Then, the LEM is combined with random field theory for slope reliability analysis considering spatially variable soil properties. Thereafter, Monte Carlo Simulation is used to evaluate the probability of slope failure. A potential pitfall of the LEM is that some assumptions relating to the shape or location of the critical failure mechanism have to be made. Also, it does not account for the stress–strain behavior of the soil. Additionally, the spatial variability of soil properties cannot be considered realistically with the LEM-based methods, unless the shape of the slip surface is non-circular (Tabarroki et al., 2013). Fortunately, finite element based methods provide solutions to overcome the aforementioned

* Corresponding author at: State Key Laboratory of Water Resources and Hydropower Engineering Science, Wuhan University, 8 Donghu South Road, Wuhan 430072, PR China. Tel.: +86 27 6877 2496; fax: +86 27 6877 4295.
E-mail address: dianqing@whu.edu.cn (D.-Q. Li).

0013-7952/$ – see front matter © 2013 Elsevier B.V. All rights reserved.
http://dx.doi.org/10.1016/j.enggeo.2013.11.006

shortcomings underlying the traditional LEM (Farias and Naylor, 1998; Griffiths and Fenton, 2004). As for the slope reliability evaluation, although the direct MCS is simple and suitable for evaluating the probability of slope failure in the presence of spatially variable shear strength parameters, the time and resources required for the MCS could be prohibitive because a substantial number of finite element model runs are needed to obtain reliability results with a sufficient accuracy. The resultant computational efforts are most pronounced at relatively small probability levels or when complex finite element analyses are needed for slope stability analysis. Traditional stochastic finite element methods require significant modification of existing deterministic numerical codes, and become nearly impossible for most engineers with no access to the source codes of commercial software packages (Ghanem and Spanos, 2003; Stefanou, 2009). Therefore, it is necessary to explore more efficient methods for slope reliability analysis, which considers spatially variable shear strength parameters and requires complex finite element analysis for determining the factor of safety.

The objective of this paper is to propose a non-intrusive stochastic finite element method for slope reliability analysis considering spatially variable shear strength parameters. To achieve this goal, this article is organized as follows. In Section 2, the two-dimensional (2-D) spatial variation of the shear strength parameters is modeled by cross-correlated non-Gaussian random fields, which are discretized by the Karhunen–Loève (KL) expansion. In Section 3, the procedure of a non-intrusive stochastic finite element method is presented. Two examples of slope reliability analysis are investigated to demonstrate the capacity and validity of the proposed method in Section 4.

2. Random field modeling of soil property

2.1. Spatial variability of soil property

A Gaussian random field is completely defined by its mean $\mu(x)$, standard deviation $\sigma(x)$, and autocorrelation function $\rho(x_1, x_2)$. The autocorrelation function is an important physical quantity for characterizing the spatial correlation of soil properties (Vanmarcke, 2010). In this study, a squared exponential 2-D autocorrelation function is adopted with different autocorrelation distances in the horizontal and vertical directions as follows:

$$\rho[(x_1,y_1),(x_2,y_2)] = \exp\left(-\left[\left(\frac{|x_1-x_2|}{l_h}\right)^2+\left(\frac{|y_1-y_2|}{l_v}\right)^2\right]\right) \tag{1}$$

where (x_1, y_1) and (x_2, y_2) are the coordinates of two arbitrary points in a 2-D space; and l_h and l_v are the autocorrelation distances in the horizontal and vertical directions, respectively.

2.2. Karhunen–Loève (KL) expansion

Several methods such as the midpoint method (Der Kiureghian and Ke, 1988), the local average subdivision (LAS) method (Vanmarcke, 2010), the shape function method (Liu et al., 1986) and the KL expansion (Phoon et al., 2002) can be used to discretize the random field. Since the KL expansion requires the minimum number of random variables for a prescribed level of accuracy, it is employed to discretize the 2-D anisotropic random fields of shear strength parameters. To facilitate the understanding of the proposed non-intrusive stochastic finite element method, the KL expansion is introduced briefly in the following.

A random field $\mathbf{H}(x, \theta)$ is a collection of random variables associated with a continuous index $x \in \Omega \subseteq R^n$, where Ω is an open set of R^n describing the system geometry and $\theta \in \Theta$ is the coordinate in the outcome space. Discretization of a random field using the KL expansion is based on the spectral decomposition of its autocorrelation function $\rho(x_1, x_2)$. Generally, the autocorrelation function is bounded, symmetric and positive definite. Hence, the discretization of a random field is defined by the eigenvalue problem of the homogenous Fredholm integral equation as follows:

$$\int_\Omega \rho(x_1,x_2) f_i(x_2)dx_2 = \lambda_i f_i(x_1) \tag{2}$$

where x_1 and x_2 denote the coordinates of two points; $f_i(\cdot)$ and λ_i are the eigenfunctions and eigenvalues of the 1-D autocorrelation function $\rho(x_1, x_2)$, respectively. Then, the eigenmodes of the separable multi-dimensional autocorrelation function are calculated by multiplying with the eigenmodes obtained from Eq. (2) (e.g., Huang, 2001).

The eigenvalue problem of the Fredholm integral equation in Eq. (2) is often solved numerically due to its complexity. The wavelet-Galerkin technique is adopted herein to solve the above eigenvalue problem. More details are given by Phoon et al. (2002). The series expansion of a 2-D random field $\mathbf{H}_i(x, y)$ is expressed as

$$\boldsymbol{H}_i(x,y) = \mu_i + \sum_{j=1}^{\infty} \sigma_i \sqrt{\lambda_j} f_j(x,y)\xi_{i,j}, \quad x,y \in \Omega \tag{3}$$

where $\xi_{i,j}$ is a set of orthogonal random coefficients (uncorrelated random variables with zero mean and unit variance). The series expansion in Eq. (3), referred to as the KL expansion, provides a second-moment characterization in terms of uncorrelated random variables and deterministic orthogonal functions. It is known to converge in the mean square sense for any distribution of $\mathbf{H}_i(x, y)$ (e.g., Vořechovský, 2008). For practical implementation, the series is approximated by a finite number of terms in Eq. (3):

$$\tilde{\boldsymbol{H}}_i(x,y) = \mu_i + \sum_{j=1}^{n} \sigma_i \sqrt{\lambda_j} f_j(x,y)\xi_{i,j}, \quad x,y \in \Omega \tag{4}$$

where n is the number of KL expansion terms to be retained, which highly depends on the desired accuracy and the autocorrelation function of the random field. Small values of the autocorrelation distances will lead to a significant increase in the number of the eigenmodes, n. Several studies (Huang, 2001; Laloy et al., 2013) took the ratio of the expected energy, ε, as a measure of the accuracy of the truncated series, which is defined as

$$\begin{aligned}\varepsilon &= \int_\Omega E\left(\tilde{\boldsymbol{H}}_i(x,y)-\mu_i\right)^2 dxdy \Big/ \int_\Omega E(\boldsymbol{H}_i(x,y)-\mu_i)^2 dxdy \\ &= \sum_{i=1}^{n}\lambda_i \Big/ \sum_{i=1}^{\infty}\lambda_i\end{aligned} \tag{5}$$

where the eigenvalues λ_i are sorted in a descending order. A large ε always indicates a high accuracy of the truncated series.

2.3. Cross-correlated non-Gaussian random fields

In geotechnical engineering practice, very often more than one geotechnical parameter needs to be modeled by random fields. Furthermore, the geotechnical engineering literature is replete with cross-correlations between two geotechnical parameters. For example, the two curve-fitting parameters underlying load–displacement curve of piles are negatively correlated (Li et al., 2013b). The cohesion and friction angle, often used for slope reliability analysis, are considered to be negatively correlated (e.g., Lumb, 1970; Wolff, 1985; Cho, 2010; Tang et al., 2013). In this case, the cross-correlated random fields need to be handled. Following Cho (2010), it is assumed that all fields simulated over a region Ω share an identical autocorrelation function over Ω, and the cross-correlation structure between each pair of simulated fields is simply defined by a cross-correlation coefficient. It can ensure that the target random fields respect the correlation structure within each field (Vořechovský, 2008). The rationale underlying these assumptions has been explained by Fenton and Griffiths (2003). Under these

assumptions, the modal decomposition of the given autocorrelation function is done only once. The same spectrum of eigenfunctions and eigenvalues can be used for the expansion of cross-correlated random fields. It should be pointed out that the sets of random variables used for the expansion of cross-correlated random fields are also cross-correlated. In the following, the cross-correlated random fields between cohesion c and friction angle ϕ are presented to illustrate the simulation procedures of cross-correlated random fields.

Denote the cross-correlation coefficient matrix between c and ϕ as $\mathbf{R}_{c,\phi} = (\rho_{c,\phi})_{2\times 2}$. The sample matrix $\boldsymbol{\xi}$ with the dimension $(n \times N_F) \times N_p$ is generated first, where N_p is the number of simulated samples, or the number of deterministic slope stability model runs; N_F is the number of random fields. Each of the N_p columns is one realization of an independent standard normal sample vector, which is partitioned into N_F vectors each with the dimension n. For the discretization of cross-correlated random fields involving two spatially variable c and ϕ, the kth column of $\boldsymbol{\xi}$, $\boldsymbol{\xi}_k = \{\xi_c^k, \xi_\phi^k\}$, $\xi_c^k = \{\xi_{c,1}^k, \xi_{c,2}^k, \cdots, \xi_{c,n}^k\}^T$, $\xi_\phi^k = \{\xi_{\phi,1}^k, \xi_{\phi,2}^k, \cdots, \xi_{\phi,n}^k\}^T$, can be performed using two sets of independent standard normal probabilistic collocation points (e.g., Li and Zhang, 2007; Li et al., 2013a) or Latin hypercube sampling points (Choi et al., 2004; Vořechovský, 2008). A lower triangular matrix $\mathbf{L}$ with a dimension of 2×2 is obtained by the Cholesky decomposition of $\mathbf{R}_{c,\phi}$. Then, the correlated standard normal sample matrix $\boldsymbol{\chi}$ is obtained. The kth column of $\boldsymbol{\chi}$, $\boldsymbol{\chi}_k$, is given by

$$\boldsymbol{\chi}_k = \left[\chi_c^k, \chi_\phi^k\right] = \boldsymbol{\xi}_k \cdot \boldsymbol{L}^T = \left[\xi_c^k, \xi_c^k \cdot \rho_{c,\phi} + \xi_\phi^k \cdot \sqrt{1-\rho_{c,\phi}^2}\right], \quad k = 1, 2, \cdots, N_p \tag{6}$$

where the matrix $\boldsymbol{\xi}_k$ with a dimension of $n \times 2$ is rearranged from the kth column of the sample matrix $\boldsymbol{\xi}$. Taking the correlated standard normal sample vector $\boldsymbol{\chi}_k$ as basis, the kth realization of each of the cross-correlated Gaussian random fields of c and ϕ is expressed as

$$\widetilde{\boldsymbol{H}}_i^{k,D} = \mu_i + \sum_{j=1}^{n} \sigma_i \sqrt{\lambda_j} f_j(x,y) \chi_{i,j}^k \quad (\text{for } i = c, \phi). \tag{7}$$

Like the isoprobabilistic transformation of non-normal random variables (e.g., Li et al., 2011), the kth realization of approximate cross-correlated non-Gaussian random fields can be obtained component-to-component,

$$\boldsymbol{H}_i^{k,NG}(x,y) = G_i^{-1}\left\{\Phi\left[\widetilde{\boldsymbol{H}}_i^{k,D}(x,y)\right]\right\} \quad (\text{for } i = c, \phi) \tag{8}$$

where $G_i^{-1}(\cdot)$ is the inverse function of marginal cumulative distribution of each component of non-Gaussian vector random field $\mathbf{H}^{NG}(x, y)$; and $\Phi(\cdot)$ is the standard Gaussian distribution function. If the shear strength parameters (c, ϕ) are considered to be lognormally distributed, the kth realization of approximate cross-correlated lognormal random fields can be obtained by exponentiating that of the approximate cross-correlated Gaussian random fields from Eq. (8) as below:

$$\boldsymbol{H}_i^{k,LN}(x,y) = \exp\left(\mu_{\ln i} + \sum_{j=1}^{n} \sigma_{\ln i} \sqrt{\lambda_j} f_j(x,y) \chi_{i,j}^k\right) \quad (\text{for } i = c, \phi) \tag{9}$$

where $\mu_{\ln i}$ and $\sigma_{\ln i}$ are the mean and standard deviation of Gaussian random variable $\ln i$, respectively, $\mu_{\ln i} = \ln \mu_i - \sigma_{\ln i}^2/2$ and $\sigma_{\ln i} = \sqrt{\ln(1 + (\sigma_i/\mu_i)^2)}$.

3. Procedure of a non-intrusive stochastic finite element method

A procedure of slope reliability analysis using a non-intrusive stochastic finite element method is proposed in this section, as shown in Fig. 1. This procedure consists of nine steps as follows:

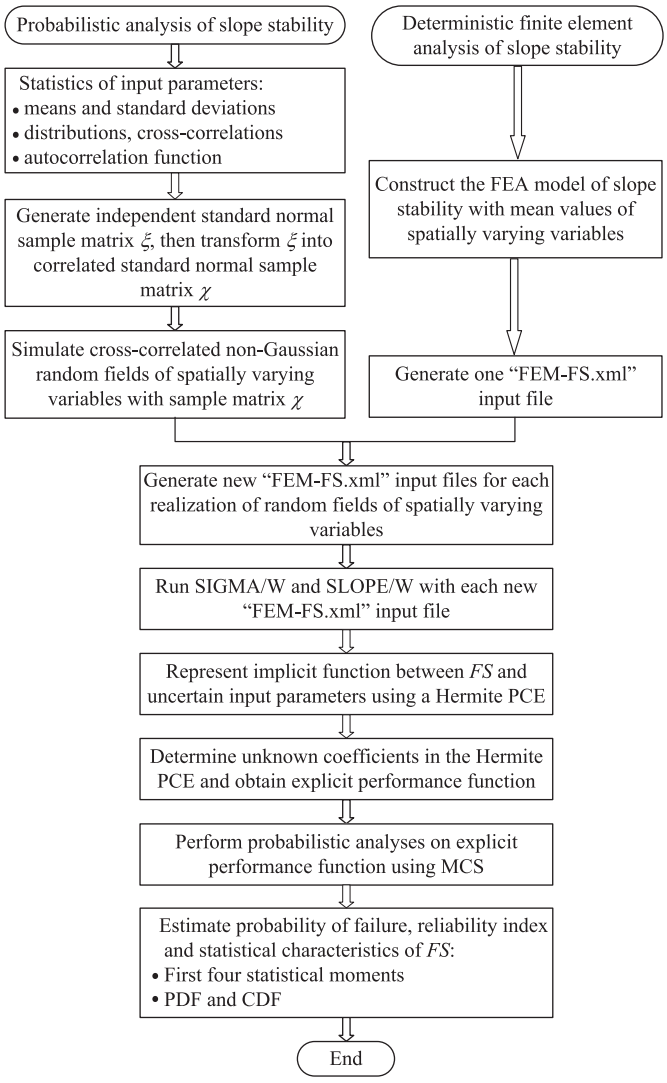

Fig. 1. Flowchart of the non-intrusive stochastic finite element method.

(1) Identify the spatially varying variables and determine their statistics such as means, coefficients of variation (COVs), distributions and cross-correlation coefficients among the variables associated with the slope reliability problem. Select an appropriate autocorrelation function and estimate the autocorrelation distances in the horizontal and vertical directions for a 2-D random field model.

(2) Construct the finite element analysis (FEA) model for slope stability analysis with the mean values of input variables using SIGMA/W and SLOPE/W (GEO-SLOPE International Ltd., 2010a, b). Then, extract the coordinates $(x_{o,i}, y_{o,i})$ of the centroid of the ith element, in which $i = 1, 2, \cdots, n_e$, n_e is the number of finite elements. Save the deterministic slope stability model file as an input file named "FEM-FS.xml". This file contains all the information needed by SIGMA/W and SLOPE/W, which can also be directly viewed via the text editor. Note that the factor of slope safety is calculated using the finite element based method (Farias and Naylor, 1998), which is implemented in SLOPE/W using the stress field obtained from finite element analysis in SIGMA/W.

(3) Generate the independent standard normal sample matrix $\boldsymbol{\xi}$ of dimension $(n \times N_F) \times N_p$ using the probabilistic collocation points or Latin hypercube sampling points. Then, transform the independent standard normal sample matrix $\boldsymbol{\xi}$ into the correlated standard normal sample matrix $\boldsymbol{\chi}$ using Eq. (6).

(4) Simulate the cross-correlated non-Gaussian random fields of spatially varying variables with the sample matrix $\boldsymbol{\chi}$ and coordinates $(x_{o,i}, y_{o,i})$ using the KL expansion in Section 2. Then, N_p realizations of cross-correlated non-Gaussian random fields of spatially varying shear strength values in the physical space are obtained, which are assigned to each finite element of the considered slope, respectively.

(5) Replace the mean values of the corresponding uncertain input parameters at the centroid of each finite element in the "FEM-FS.xml" file generated in step (2) with each pair of spatially varying variables (i.e., c and ϕ) in each realization of random fields in step (4). Then, N_p different new "FEM-FS.xml" input files are generated. In this manner, no programming effort is required to modify the existing finite element code compared with the spectral stochastic finite element method (Ghanem and Spanos, 2003).

(6) Run SIGMA/W and SLOPE/W with each new "FEM-FS.xml" input file generated in step (5) to perform deterministic FEA of slope stability. Such a process can be executed automatically with the help of Winbatch™. Winbatch™ is a Microsoft Windows scripting language and possesses an optional compiler used to create self-contained executables. This process will produce N_p different factors of slope safety, $FS = (FS_1, FS_2, \ldots, FS_{Np})$, which can be directly extracted from the corresponding result files named "FEM-FS.fac".

(7) Replace the implicit function between the factor of slope safety, FS, and the uncertain input parameters by a Hermite polynomial chaos expansion (PCE) called meta-model when the FEA of slope stability is involved (Isukapalli et al., 1998; Ghanem and Spanos, 2003). The PCE methodology has been widely used in geotechnical engineering (Li et al., 2011; Mollon et al., 2011; Al-Bittar and Soubra, 2013).

$$\begin{aligned} FS(\boldsymbol{\xi}) = a_0\Gamma_0 &+ \sum_{i_1=1}^{N} a_{i_1}\Gamma_1\left(\xi_{i_1}\right) + \sum_{i_1=1}^{N}\sum_{i_2=1}^{i_1} a_{i_1 i_2}\Gamma_2\left(\xi_{i_1},\xi_{i_2}\right) \\ &+ \sum_{i_1=1}^{N}\sum_{i_2=1}^{i_1}\sum_{i_3=1}^{i_2} a_{i_1 i_2 i_3}\Gamma_3\left(\xi_{i_1},\xi_{i_2},\xi_{i_3}\right) \\ &+ \cdots + \sum_{i_1=1}^{N}\sum_{i_2=1}^{i_1}\sum_{i_3=1}^{i_2}\cdots\sum_{i_N=1}^{i_{N-1}} a_{i_1 i_2,\cdots,i_N}\Gamma_N\left(\xi_{i_1},\xi_{i_2},\cdots,\xi_{i_N}\right) \end{aligned} \tag{10}$$

where N is the total number of random variables, $N = n \times N_F$; $\boldsymbol{a} = \left(a_0, a_{i_1}, \cdots, a_{i_1 i_2,\cdots,i_N}\right)$ are the unknown coefficients to be evaluated; $\boldsymbol{\xi}_i = \left(\xi_{i_1}, \xi_{i_2}, \cdots, \xi_{i_N}\right)$ is the vector of independent standard normal variables representing the uncertainties in the input parameters, which corresponds to the random variables used to discretize the random fields using the KL expansion in Eq. (3); and $\Gamma_N\left(\xi_{i_1}, \xi_{i_2}, \cdots, \xi_{i_N}\right)$ are the multidimensional Hermite polynomials of degree N. The reader is referred to Ghanem and Spanos (2003) and Li et al. (2011) for details. Note that the number of unknown coefficients in Eq. (10) is N_c, $N_c = (N + p)!/(N! \times p!)$ for the pth order PCE.

(8) Determine the unknown coefficients in the Hermite PCE by equating the factors of safety obtained from step (6) with the estimates from the series approximation in Eq. (10) at the matrix $\boldsymbol{\xi}$ from step (3), then constructing and solving a system of linear equations. The collocation method based on the linearly independent principle (Li and Zhang, 2007) or the regression based approach (Isukapalli et al., 1998) can be used for such purpose. Then, the explicit function between FS and the uncertain input parameters is obtained.

(9) Perform probabilistic analyses on the explicit performance function $G(\boldsymbol{\xi}) = FS(\boldsymbol{\xi}) - 1$. The probability of failure and the corresponding reliability index can be estimated by using the MCS with one million samples on the performance function with the FS represented by a Hermite PCE. The first four statistical moments can also be directly evaluated using the PCE (Mollon et al., 2011). It should be pointed out that the evaluation of the performance function does not require deterministic FEA of slope stability again, but only involve the evaluation of simple algebraic expressions, which is much more computationally efficient.

4. Illustrative examples

4.1. Application to a saturated clay slope under undrained conditions ($\phi_u = 0$)

In the first example, an undrained clay slope studied by Griffiths and Fenton (2004) and Cho (2010) is investigated. A typical finite element model of the considered slope is shown in Fig. 2. The majority of the elements are squares and the elements adjacent to the slope surface are degenerated into triangles. The types of elements are 4-node quadrilateral elements and 3-node triangular elements. In Fig. 2, the finite element mesh consists of 910 elements and 981 nodes. For illustrative purposes, a conventional elastic and perfectly plastic model based on the Mohr–Coulomb failure criterion is adopted to represent the stress–strain behavior of the soil. The boundary conditions are rollers on both lateral boundaries and full fixity at the base.

To avoid negative values, the undrained shear strength, c_u, is considered as a log-normally distributed random field. Table 1 summarizes the statistical properties of soil parameters for the considered slope. Note that Young's modulus E, Poisson's ratio v, and unit weight γ_{sat} of the soil are treated as deterministic quantities because their variations are relatively low compared with c_u (Duncan, 2000). Based on the mean value of the undrained shear strength, the minimum factor of slope safety is obtained as 1.366 using the finite element based method based on the search algorithm for the critical failure surface, which is implemented in SIGMA/W and SLOPE/W. The corresponding critical failure surface is plotted in Fig. 2, which is deep and passes through the foundation soil. For comparison, the factor of safety using the limit equilibrium method is also calculated for this slope model. The FS is 1.354 using the Morgenstern–Price method, which is consistent with 1.356 using Bishop's simplified method reported in Cho (2010). These results indicate that the finite element based method adopted in this study evaluates the slope stability problem effectively.

For computational efficiency, the KL expansion is employed to discretize the 2-D log-normally distributed random field of c_u. The accuracy of discretization of random field highly depends on the number of eigenmodes, n. Generally, an increase in the number of eigenmodes increases the accuracy. However, it also increases the computational effort. In practice, a compromise between accuracy and computational cost is achieved by accepting some amount of error. The wavelet-Galerkin technique is used herein to solve the eigenvalue problem underlying the squared exponential autocorrelation function in Eq. (1). Fig. 3 shows the decaying trends of the eigenvalues obtained by solving the integral eigenvalue problem. Note that the eigenvalues decay drastically with the number of KL terms. Moreover, the rate of decay increases with increasing autocorrelation distance. For $n = 10$, the ratios of the expected energy in Eq. (5) are 92.8%, 97.1% and 98.7% for ($l_h = 20$ m, $l_v = 2$ m), ($l_h = 25$ m, $l_v = 2.5$ m) and ($l_h = 30$ m, $l_v = 3$ m), respectively. When n increases from 10 to 15 associated with ($l_h = 25$ m, $l_v = 2.5$ m), the ratio of the expected energy, ε, only increases from 97.1% to 99.3%. The improvement in the ratio of the expected energy is less significant. However, the resulting computational effort is increased significantly in comparison with that for $n = 10$. A ratio of $\varepsilon \geq 95\%$ is commonly taken as a criterion for determining the number of eigenmodes n (Laloy et al., 2013). Taking the autocorrelation distances of $l_h = 25$ m and $l_v = 2.5$ m as an example, which are typical values reported in the literature (Phoon and Kulhawy, 1999; El-Ramly et al., 2003), a value of $n = 10$ is adopted to achieve a compromise between accuracy and efficiency in the following.

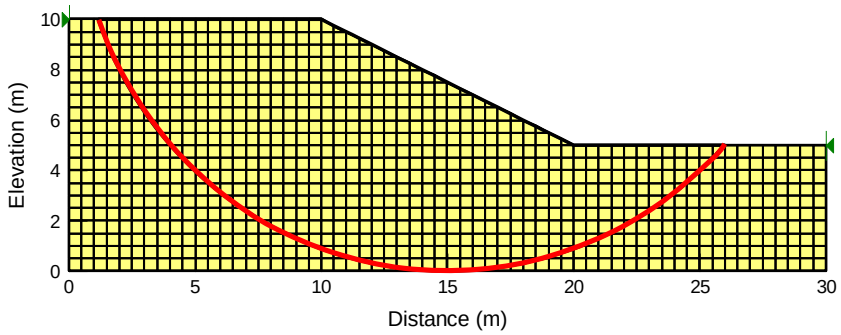

Fig. 2. FEM model of the homogeneous undrained clay slope with $FS = 1.366$.

The finite element size is an important parameter which can affect the accuracy of reliability results when the spatial variability is considered. As suggested by Griffiths and Fenton (2004) and Ching and Phoon (2013), the ratio of the element size to the scale of fluctuation has to be sufficiently small to ensure that the variance function approaches 1.0. For the autocorrelation distances of $l_h = 25$ m and $l_v = 2.5$ m, the ratio of the element size to the vertical scale of fluctuation, $\frac{\Delta z}{\delta_v} = \frac{0.5}{2.5\sqrt{\pi}} = 0.11$, is relatively small for a square finite element of side length 0.5 m. It can be seen from Vanmarcke (1977) that the variance function $\Gamma_u(\Delta z)$ approaches 1.0 when the spatial autocorrelation is modeled by the squared exponential model. This also agrees with the observation in Ching and Phoon (2013) that the element size has to be smaller than $0.13\delta_v$ to $0.17\delta_v$ depending on the stress states and failure curve orientations when the squared exponential autocorrelation function is adopted. Although a finer mesh can produce better estimates of factor of slope safety and probability of slope failure, the resulting computational time increases dramatically. To strike balance between accuracy and computational cost, the 4-node quadrilateral elements and 3-node triangular elements with an element size of 0.5 m are adopted in this study. Additionally, the finite element mesh should be changed along with the autocorrelation distance.

To obtain the random field realizations of spatially variable c_u, an independent standard normal sample matrix $\boldsymbol{\xi}$ with dimensions of 10×66 is first generated for the 2nd order Hermite PCE using the probabilistic collocation points (e.g., Li et al., 2011). This sample matrix, $\boldsymbol{\xi}_{10\times 66}$, and coordinates $(x_{o,i}, y_{o,i})$, in which $i = 1, 2, \cdots, 910$, are used to simulate the lognormal random field of c_u. Then, a parameter matrix of spatially variable c_u with dimensions of 910×66 in the physical space is obtained from the KL expansion. These 910 values of c_u in each column of the parameter matrix are assigned to each finite element according to the order of coordinates $(x_{o,i}, y_{o,i})$. By replacing the mean values of c_u for each finite element in the original "FEM-FS.xml" file with these 910 values of c_u, a new "FEM-FS.xml" input file is generated. Applying the similar method, 66 different new "FEM-FS.xml" input files can be obtained. The deterministic FEA of slope stability is carried out based on these 66 new "FEM-FS.xml" input files via SIGMA/W and SLOPE/W. This process will produce 66 different factors of slope safety, $FS = (FS_1, FS_2, \ldots, FS_{66})$, which are extracted from the corresponding result files named "FEM-FS.fac", respectively. The explicit function between the factor of slope safety and independent standard normal variables is constructed using the 2nd order Hermite PCE. A system of linear equations is constructed by equating the factors of safety obtained from the 66 runs of deterministic finite element slope stability analysis with the estimates from the series approximation in Eq. (10). The unknown coefficients in the 2nd order Hermite PCE can be determined using the collocation point method based on the linearly independent principle (e.g., Li and Zhang, 2007; Li et al., 2013a). Finally, the probability of slope failure is obtained as 11.8% using the direct MCS with 10^6 samples. Similarly, the probability of slope failure is obtained as 11.56% from the 3rd order Hermite PCE where the independent standard normal sample matrix $\boldsymbol{\xi}$ with dimensions of 10×286 is used. Note that the direct MCS are carried out on the explicit performance function represented by the Hermite PCE. The calculation of FS does not involve finite element model runs, but only the evaluation of simple algebraic expressions, which is much more computationally efficient.

Table 2 shows the reliability results of an undrained clay slope for autocorrelation distances of $l_h = 25$ m, $l_v = 2.5$ m using the proposed non-intrusive stochastic finite element method. To validate the proposed method, the results obtained from the LHS with 1000 simulations are also provided in Table 2. The coefficient of variation of the probability of failure, p_f, associated with the LHS, $COV_{p_f} = \sqrt{(1-p_f)/(1000 \cdot p_f)}$ (e.g., Zhang et al., 2013), is 8.9% and 6.8% for $l_h = 25$ m, $l_v = 2.5$ m ($p_f = 11.2\%$) and $l_h = 1000$ m, $l_v = 1000$ m ($p_f = 17.6\%$), respectively. They are smaller than the commonly used value 10% in the literature. Thus, the results obtained from the LHS with 1000 simulations can be taken as "exact" solutions for this example. The probabilities of failure obtained from the 2nd and 3rd order PCEs are 11.8% and 11.56%, respectively. The corresponding relative errors in the probability of failure are 5.4% and 3.2% in comparison with 11.2% obtained from the LHS method. These results indicate that the proposed method can produce sufficiently accurate probability of failure. Additionally, the numbers of finite element model runs, N_p, for the 2nd and 3rd order PCEs are 66 and 286

Table 1
Statistical properties of soil parameters for an undrained clay slope.

Parameter	Mean	COV
Undrained shear strength c_u (kPa)	23	0.3
Young's modulus E (MPa)	100	–
Poisson's ratio ν	0.3	–
Unit weight γ_{sat} (kN/m^3)	20	–

Note: The symbol "–" denotes that the parameter is constant.

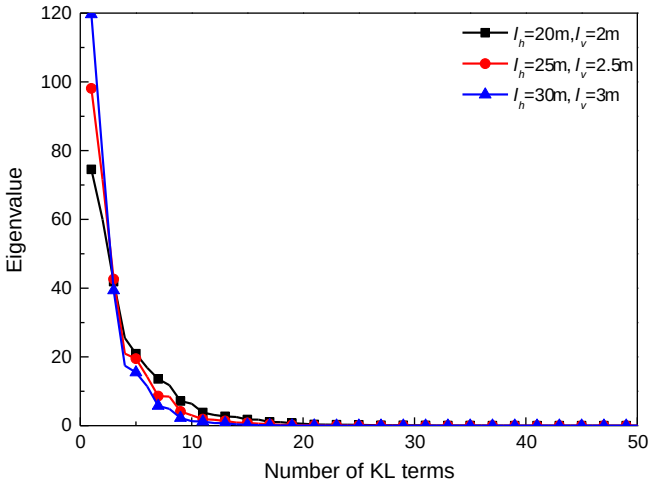

Fig. 3. Eigenvalues of the autocorrelation function.

Table 2
Reliability results of an undrained clay slope for $l_h = 25$ m and $l_v = 2.5$ m.

Method	μ_{FS}	σ_{FS}	δ_{FS}	κ_{FS}	p_f (%)	β
2nd order PCE ($N_p = 66$)	1.272	0.243	0.457	3.520	11.80	1.185
3rd order PCE ($N_p = 286$)	1.312	0.303	0.814	5.501	11.56	1.197
LHS ($N_p = 1000$)	1.294	0.252	0.586	3.568	11.20	1.216

Table 3
Reliability results of an undrained clay slope for $l_h = 1000$ m and $l_v = 1000$ m.

Method	μ_{FS}	σ_{FS}	δ_{FS}	κ_{FS}	p_f (%)	β
2nd order PCE ($N_p = 66$)	1.372	0.411	0.834	3.933	18.52	0.896
3rd order PCE ($N_p = 286$)	1.371	0.411	0.921	4.490	17.65	0.929
LHS ($N_p = 1000$)	1.372	0.412	0.916	4.430	17.60	0.931
SRV	1.366	0.414	–	–	17.95	0.917

Note: SRV denotes the single random variable approach.

based on the rank of the information matrix, respectively, which are just equal to the number of unknown coefficients in the Hermite PCE, N_c. In contrast, the LHS needs 1000 finite element model runs to achieve a reasonable accuracy. It is evident that the non-intrusive stochastic finite element method is much more efficient than the LHS method. The first four statistical moments of the factor of safety are also listed in Table 2. The computed skewness and kurtosis using the LHS with 1000 simulations are 0.586 and 3.568, respectively. These values are 0 and 3 for a normal distribution, which suggests that the factor of safety of the undrained clay slope as a random variable does not follow a normal distribution.

Similarly, Table 3 shows the reliability results of an undrained clay slope for autocorrelation distances of $l_h = 1000$ m and $l_v = 1000$ m. The probabilities of failure obtained from the 2nd and 3rd order PCEs are 18.52% and 17.65%, respectively. Taking 17.6% obtained from the LHS with 1000 simulations as the "exact" solution, the relative errors associated with the 2nd and 3rd order PCEs are 5.2% and 0.3%, respectively. When the undrained shear strength is modeled by a single random variable, the probability of slope failure is 17.95% using the approach presented in Griffiths and Fenton (2004), which is almost identical to that obtained from the random field model with the autocorrelation distances of $l_h = 1000$ m and $l_v = 1000$ m. Such result clearly indicates that when only the probability of failure is of great interest, the random field model with the autocorrelation distances of $l_h = 1000$ m and $l_v = 1000$ m is almost equivalent to the single random variable model. With regard to the computational efficiency, the numbers of finite element model runs for the 2nd and 3rd order PCEs are 66 and 286, respectively. The computational cost for the 2nd order PCE is only about one quarter of that for the 3rd order PCE. Hence, the non-intrusive stochastic finite element method with a 2nd order PCE is used in the subsequent analyses.

Fig. 4 summarizes the variations of the probability of slope failure with the coefficient of variation of c_u (COVc_u) for various factors of slope safety. The autocorrelation distances of $l_h = 1000$ m and $l_v = 1000$ m represent the case of ignoring spatial variation in c_u. It can be observed that ignoring spatial variation will lead to unconservative estimate of the probability of slope failure if *FS* is below 1.0. This result contradicts with the findings of other investigators who used classical slope reliability analysis tools (e.g., Cho, 2007; Cho, 2010; Griffiths et al., 2011). With the increase of *FS*, there are crossover points between the curves associated with ($l_h = 25$ m, $l_v = 2.5$ m) and ($l_h = 1000$ m, $l_v = 1000$ m), which give a critical value of COVc_u. When the COVc_u exceeds the critical value, ignoring spatial variation in c_u will underestimate the probability of slope failure. Such findings are consistent with the observations reported in Griffiths and Fenton (2004). Additionally, the critical value of COVc_u increases with increasing *FS*. An important observation highlighted in Fig. 4 is that a $FS = 1.3$ for the considered slope would lead to a probability of failure as high as $p_f = 18\%$ associated with COV$c_u = 0.3$ and ($l_h = 25$ m, $l_v = 2.5$ m). In geotechnical engineering practice, however, slopes with a factor of safety as high as $FS = 1.3$ rarely fail. These results further support the conclusions drawn by Duncan (2000). He stated that "Computing both factor of safety and probability of failure is better than computing either one alone. Although neither factor of safety nor probability of failure can be computed with high precision, both have value and each enhances the value of the other".

Another interesting finding observed from Fig. 4 is that the probability of slope failure associated with $FS < 1$ does always increases with COVc_u in comparison with $FS > 1$. This is because for a relatively small *FS*, the mean value of c_u has a more significant influence on the probability of slope failure compared with the COVc_u. To further explain this finding, Fig. 5 shows the probabilities of slope failure for various values of COVc_u and *FS* using the single random variable approach. The probabilities of slope failure increase with COVc_u for a relative high *FS*. When *FS* is below 0.96, however, COV$c_u = 0.1$ leads to higher probabilities of slope failure than those associated with COVc_u exceeding 0.1.

4.2. Application to a c–ϕ slope

In the second example, the stability of a c–ϕ slope studied by Griffiths and Fenton (2004) is investigated again. Like the first example, a typical finite element model of the considered c–ϕ slope is presented in Fig. 6. The finite element mesh is identical to that in Fig. 2, which can also lead to almost no variance reduction when the squared exponential autocorrelation model with autocorrelation distances of $l_h = 25$ m and

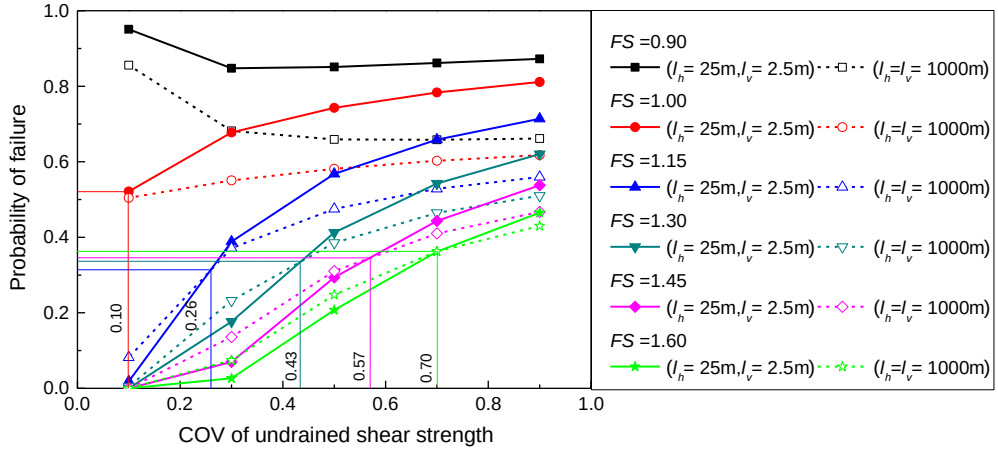

Fig. 4. Probabilities of failure for various COVs of undrained shear strength and factors of safety.

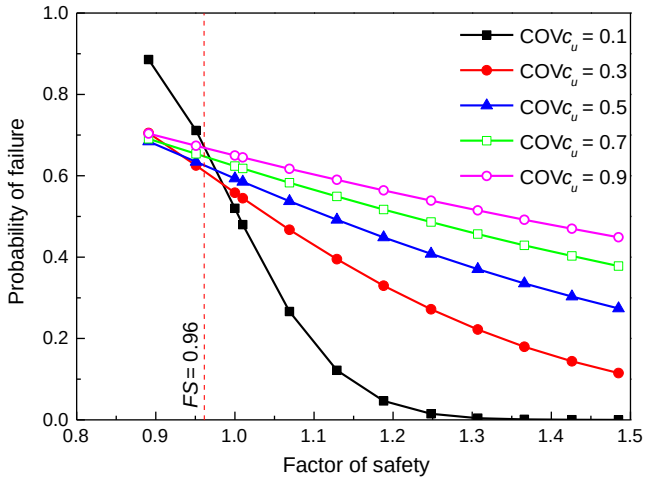

Fig. 5. Effect of *FS* on probability of failure for various COVs of undrained shear strength using single random variable model.

$l_v = 2.5$ m is adopted. Table 4 summarizes the statistical properties of the soil parameters for the c–ϕ slope. The cohesion and friction angle are modeled as cross-correlated lognormal random fields. Again, Young's modulus E, Poisson's ratio v and unit weight γ are treated as deterministic quantities. The critical failure surface obtained from the deterministic analysis passes the slope toe, which is significantly different from that for the undrained clay slope in Fig. 2. Using the mean values of the cohesion and friction angle, the minimum factor of safety of the c–ϕ slope is 1.780 from the finite element analysis incorporating an automatic search algorithm. Also, the coordinates of the centroids of 910 finite elements are extracted and this deterministic slope stability model file is saved as an input file named "FEM-FS.xml".

Unlike the first example, 20 independent standard normal random variables are needed to discretize cross-correlated lognormal random fields of c and ϕ when a value of $n = 10$ is selected for each spatially varying variable. The sample matrix, $\boldsymbol{\xi}$, with dimensions of 20×462 is first generated for the 2nd order Hermite PCE using the Latin hypercube sampling points (Choi et al., 2004). The number of samples, 462, is used because it is twice the number of coefficients, N_c, based on the regression based approach (Isukapalli et al., 1998). Then, the independent standard normal sample matrix, $\boldsymbol{\xi}$, is transformed into the correlated standard normal sample matrix, $\boldsymbol{\chi}$, using Eq. (6) by the Cholesky decomposition of $\mathbf{R}_{c,\phi}$. The sample matrix $\boldsymbol{\chi}_{20 \times 462}$ and coordinates $(x_{o,i}, y_{o,i})$, in which $i = 1, 2, \cdots, 910$, are used to simulate the 2-D cross-correlated lognormal random fields of c and ϕ using Eqs. (6)–(9). Two parameter matrices of spatially variable c and ϕ in which each has dimensions of 910×462 in the physical space are obtained using the KL expansion. These 910 pairs of values of c and ϕ in each column of the parameter matrices are assigned to each finite element according to the order of coordinates $(x_{o,i}, y_{o,i})$. Like the first example, 462 different

Table 4
Statistical properties of soil parameters for a c–ϕ slope.

Parameter	Mean	COV
Cohesion c (kPa)	10	0.3
Friction angle ϕ (°)	20	0.2
Young's modulus E (MPa)	100	–
Poisson's ratio ν	0.3	–
Unit weight γ (kN/m^3)	20	–

new "FEM-FS.xml" input files and the corresponding factors of slope safety, $FS = (FS_1, FS_2, \ldots, FS_{462})$, can be obtained. Finally, the unknown coefficients in the 2nd order Hermite PCE are determined using the regression based approach. Similarly, the probability of slope failure can also be obtained using direct MCS with 10^6 samples.

Table 5 shows the reliability results of a c–ϕ slope for autocorrelation distances of $l_h = 25$ m and $l_v = 2.5$ m and $\rho_{c,\phi} = 0$. The probabilities of failure obtained from the 2nd order PCEs with 462 and 2500 runs of finite element model are 6.26E-4 and 4.32E-4, respectively. This low probability of failure is often required in most geotechnical structures management demands and corresponds to the practical cases. However, for the same problem, the MCS requires more than one million runs of finite element model to produce sufficiently accurate results when the coefficient of variation of p_f below 10% is satisfied. This is almost impossible for complex slope reliability problems. In Table 5, the results obtained from the 2nd order PCE are consistent with those obtained from 3rd order PCE. Taking the reliability index for the 3rd order PCE as the "exact" solution, the relative error in reliability index for the 2nd order PCE is below 5.0%, which indicates that the 2nd order PCE has converged and can produce satisfactory results based on the convergence property of the PCE (Mollon et al., 2011; Li et al., 2013a). For computational efficiency, the 2nd order PCE is also employed in the following.

To account for the effect of cross-correlation between cohesion and friction angle on the slope reliability, the cross-correlation coefficient $\rho_{c,\phi}$ is needed. Several studies (Lumb, 1970; Wolff, 1985; Tang et al., 2012) reported values of $\rho_{c,\phi}$. The range of $-0.5 \le \rho_{c,\phi} \le 0.5$ is used in this study for illustration. Fig. 7 compares the probabilities of slope failure for the random field approach with autocorrelation distances of $l_h = 25$ m and $l_v = 2.5$ m and the random variable approach. The cross-correlation between c and ϕ has a significant influence on the probability of slope failure. For the autocorrelation distances of $l_h = 25$ m and $l_v = 2.5$ m, the probability of failure changes several orders of magnitude (i.e., increasing from 3.0E-06 to 4.97E-03) when $\rho_{c,\phi}$ varies from -0.5 to 0.5. As expected, the probability of slope failure decreases when the negative cross-correlation becomes stronger and increases with positive cross-correlation coefficient. Therefore, the probability of failure under the assumption of independence between c and ϕ may be severely biased if the actual cross-correlation is positive or negative. It can also be noted that the random variable approach

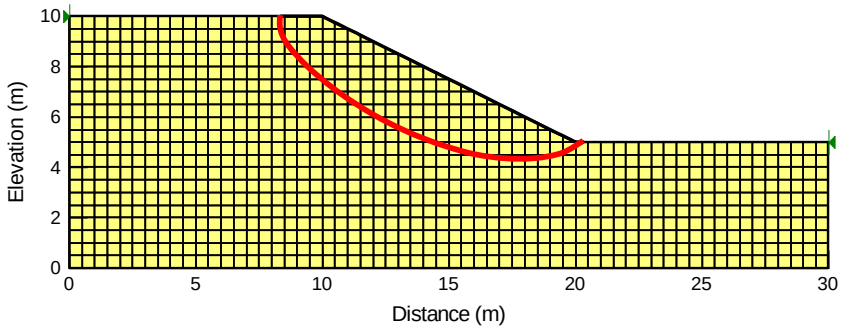

Fig. 6. FEM model of the homogeneous c–ϕ slope with $FS = 1.780$.

Table 5
Reliability results of a c–ϕ slope for $l_h = 25$ m and $l_v = 2.5$ m.

Method	μ_{FS}	σ_{FS}	δ_{FS}	κ_{FS}	p_f (%)	β
2nd order PCE ($N_p = 462$)	1.721	0.227	0.171	3.175	6.26E-4	3.227
2nd order PCE ($N_p = 2500$)	1.721	0.228	0.243	3.185	4.32E-4	3.331
3rd order PCE ($N_p = 2500$)	1.721	0.236	0.323	3.286	3.55E-4	3.386

underestimates the probability of failure for large positive correlation coefficient between cohesion and friction angle, which is consistent with the observation in Griffiths et al. (2011).

5. Conclusions

A non-intrusive stochastic finite element method has been proposed for slope reliability analysis considering spatial variability of shear strength parameters. The KL expansion is adopted to discretize the 2-D cross-correlated non-Gaussian random fields of spatially variable shear strength parameters. Two illustrative examples of slope reliability analysis are investigated to demonstrate the capacity and validity of the proposed method. Several conclusions are drawn from this study:

(1) The proposed method does not require the user to modify existing deterministic finite element codes. Moreover, the deterministic finite element analysis and the probabilistic analysis are decoupled. The proposed method provides a practical tool for reliability problems involving complex finite element analysis.
(2) The non-intrusive stochastic finite element method can efficiently evaluate the slope reliability in the presence of spatial variability in shear strength parameters. It can reduce the number of calls to the deterministic finite element model substantially and is much more efficient than the LHS method. Additionally, this method can yield satisfactory results for low failure risk corresponding to most practical cases.
(3) Ignoring spatial variability of shear strength parameters will result in unconservative estimates of the probability of slope failure if the coefficients of variation of shear strength parameters exceed a critical value or the factor of slope safety is relatively low. The critical coefficient of variation of shear strength parameters increases with increasing the factor of slope safety.
(4) The variation of probability of slope failure highly depends on the factor of slope safety. The lower the value of factor of safety (i.e., $FS = 0.9$ in the first example), the more likely it is that the shear strength parameters with low variability will overestimate the probability of slope failure, which is conservative for slope safety assessment.
(5) When the spatial autocorrelation of the shear strength parameters is very weak, more KL expansion terms are needed to produce sufficiently accurate reliability results. In order to improve the computational efficiency, other high efficient polynomial chaos expansions such as the sparse polynomial chaos expansion should be incorporated into the non-intrusive stochastic finite element method.

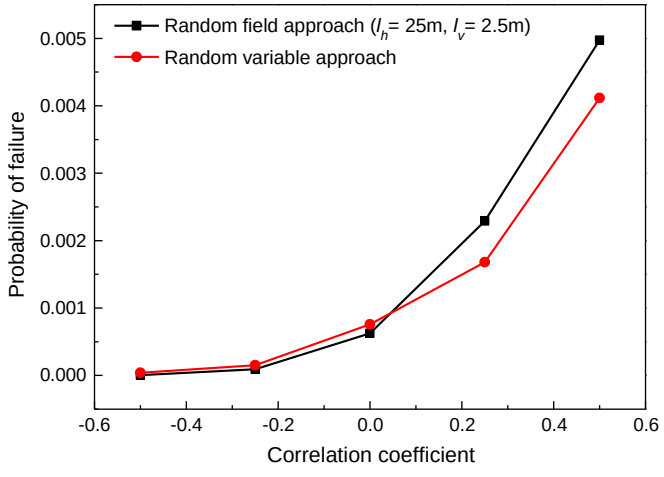

Fig. 7. Effect of cross-correlation between cohesion and friction angle on probability of failure.

Acknowledgments

This work was supported by the National Science Fund for Distinguished Young Scholars (Project No. 51225903), the National Basic Research Program of China (973 Program) (Project No. 2011CB013506) and the National Natural Science Foundation of China (Project No. 51329901).

References

Al-Bittar, T., Soubra, A.-H., 2013. Bearing capacity of strip footings on spatially random soils using sparse polynomial chaos expansion. Int. J. Numer. Anal. Methods Geomech. 37 (13), 2039–2060.
Ching, J., Phoon, K.K., 2013. Effect of element sizes in random field finite element simulations of soil shear strength. Comput. Struct. 126, 120–134.
Cho, S.E., 2007. Effects of spatial variability of soil properties on slope stability. Eng. Geol. 92 (3–4), 97–109.
Cho, S.E., 2010. Probabilistic assessment of slope stability that considers the spatial variability of soil properties. J. Geotech. Geoenviron. 136 (7), 975–984.
Cho, S.E., 2012. Probabilistic analysis of seepage that considers the spatial variability of permeability for an embankment on soil foundation. Eng. Geol. 133–134, 30–39.
Choi, S.K., Canfield, R., Grandhi, R., Pettit, C., 2004. Polynomial chaos expansion with Latin hypercube sampling for estimating response variability. AIAA J. 42 (6), 1191–1198.
Der Kiureghian, A., Ke, J.-B., 1988. The stochastic finite element method in structural reliability. Probabilistic Eng. Mech. 3 (2), 83–91.
Duncan, J.M., 2000. Factors of safety and reliability in geotechnical engineering. J. Geotech. Geoenviron. 126 (4), 307–316.
El-Ramly, H., Morgenstern, N.R., Cruden, D.M., 2003. Probabilistic stability analysis of a tailings dyke on presheared clay-shale. Can. Geotech. J. 40 (1), 192–208.
Farias, M.M., Naylor, D.J., 1998. Safety analysis using finite elements. Comput. Geotech. 22 (2), 165–181.
Fenton, G.A., Griffiths, D.V., 2003. Bearing capacity prediction of spatially random c–φ soils. Can. Geotech. J. 40 (1), 54–65.
GEO-SLOPE International Ltd., 2010a. Stress–Deformation Modeling with SIGMA/W 2007 Version: An Engineering Methodology [Computer Program]. GEO-SLOPE International Ltd., Calgary, Alberta, Canada.
GEO-SLOPE International Ltd., 2010b. Stability Modeling With SLOPE/W 2007 Version: An Engineering Methodology [Computer Program]. GEO-SLOPE International Ltd., Calgary, Alberta, Canada.
Ghanem, R.G., Spanos, P.D., 2003. Stochastic Finite Element: A Spectral Approach. Revised version Dover Publication, Inc., Mineola, New York.
Griffiths, D.V., Fenton, G.A., 2004. Probabilistic slope stability analysis by finite elements. J. Geotech. Geoenviron. 130 (5), 507–518.
Griffiths, D.V., Huang, J.S., Fenton, G.A., 2011. Probabilistic infinite slope analysis. Comput. Geotech. 38 (4), 577–584.
Huang, S.P., 2001. Simulation of Random Processes Using Karhunen–Loeve Expansion. (Ph.D. thesis) National University of Singapore, Singapore.
Isukapalli, S.S., Roy, A., Georgopoulos, P.G., 1998. Stochastic response surface methods for uncertainty propagation: application to environmental and biological systems. Risk Anal. 18 (3), 351–363.
Ji, J., Liao, H.J., Low, B.K., 2012. Modeling 2-D spatial variation in slope reliability analysis using interpolated autocorrelations. Comput. Geotech. 40, 135–146.
Laloy, E., Rogiers, B., Vrugt, J.A., Mallants, D., Jacques, D., 2013. Efficient posterior exploration of a high-dimensional groundwater model from two-stage MCMC simulation and polynomial chaos expansion. Water Resour. Res. 49 (5), 2664–2682.
Li, H., Zhang, D., 2007. Probabilistic collocation method for flow in porous media: comparisons with other stochastic method. Water Resour. Res. 43 (W09409), 44–48.
Li, D.Q., Chen, Y.F., Lu, W.B., Zhou, C.B., 2011. Stochastic response surface method for reliability analysis of rock slopes involving correlated non-normal variables. Comput. Geotech. 38 (1), 58–68.
Li, D.Q., Jiang, S.H., Chen, Y.G., Zhou, C.B., 2013a. A comparative study of three collocation point methods for odd order stochastic response surface method. Struct. Eng. Mech. 45 (5), 595–611.
Li, D.Q., Tang, X.S., Phoon, K.K., Chen, Y.F., Zhou, C.B., 2013b. Bivariate simulation using copula and its application to probabilistic pile settlement analysis. Int. J. Numer. Anal. Methods Geomech. 37 (6), 597–617.
Li, D.Q., Qi, X.H., Phoon, K.K., Zhang, L.M., Zhou, C.B., 2013c. Effect of spatially variable shear strength parameters with linearly increasing mean trend on reliability of infinite slopes. Struct. Saf.. http://dx.doi.org/10.1016/j.strusafe.2013.08.005.
Liu, W.K., Belytschko, T., Mani, A., 1986. Random field finite elements. Int. J. Numer. Methods Eng. 23 (10), 1831–1845.

Low, B.K., Lacasse, S., Nadim, F., 2007. Slope reliability analysis accounting for spatial variation. Georisk 1 (4), 177–189.
Lumb, P., 1970. Safety factors and the probability distribution of soil strength. Can. Geotech. J. 7 (3), 225–242.
Mollon, G., Dias, D., Soubra, A.-H., 2011. Probabilistic analysis of pressurized tunnels against face stability using collocation-based stochastic response surface method. J. Geotech. Geoenviron. 137 (4), 385–397.
Phoon, K.K., Kulhawy, F.H., 1999. Characterization of geotechnical variability. Can. Geotech. J. 36 (4), 612–624.
Phoon, K.K., Huang, S.P., Quek, S.T., 2002. Implementation of Karhunen–Loeve expansion for simulation using a wavelet-Galerkin scheme. Probabilistic Eng. Mech. 17 (3), 293–303.
Srivastava, A., Sivakumar Babu, G.L., 2009. Effect of soil variability on the bearing capacity of clay and in slope stability problems. Eng. Geol. 108 (1–2), 142–152.
Srivastava, A., Sivakumar Babu, G.L., Haldar, S., 2010. Influence of spatial variability of permeability property on steady state seepage flow and slope stability analysis. Eng. Geol. 110 (3–4), 93–101.
Stefanou, G., 2009. The stochastic finite element method: past, present and future. Comput. Methods Appl. Mech. Eng. 198 (9–12), 1031–1051.
Tabarroki, M., Ahmad, F., Banaki, R., Jha, S., Ching, J., 2013. Determining the factors of safety of spatially variable slopes modeled by random fields. J. Geotech. Geoenviron. 139 (12), 2082–2095.
Tang, X.S., Li, D.Q., Chen, Y.F., Zhou, C.B., Zhang, L.M., 2012. Improved knowledge-based clustered partitioning approach and its application to slope reliability analysis. Comput. Geotech. 45, 34–43.
Tang, X.S., Li, D.Q., Rong, G., Phoon, K.K., Zhou, C.B., 2013. Impact of copula selection on geotechnical reliability under incomplete probability information. Comput. Geotech. 49, 264–278.
Vanmarcke, E.H., 1977. Probabilistic modeling of soil profiles. J. Geotech. Eng. Div. 103 (11), 1227–1246.
Vanmarcke, E.H., 2010. Random Fields: Analysis and Synthesis. Revised and Expanded New Edition. World Scientific Publishing, Beijing.
Vořechovský, M., 2008. Simulation of simply cross-correlated random fields by series expansion methods. Struct. Saf. 30 (4), 337–363.
Wang, Y., Cao, Z.J., Au, S.K., 2011. Practical reliability analysis of slope stability by advanced Monte Carlo simulations in a spreadsheet. Can. Geotech. J. 48 (1), 162–172.
Wolff, T.F., 1985. Analysis and Design of Embankment Dam Slopes: A Probabilistic Approach. (Ph. D. thesis) Purdue University, Lafayette, Ind, USA.
Zhang, J., Huang, H.W., Juang, C.H., Li, D.Q., 2013. Extension of Hassan and Wolff method for system reliability analysis of soil slopes. Eng. Geol. 160, 81–88.
Zhu, H., Zhang, L.M., 2013. Characterizing geotechnical anisotropic spatial variations using random field theory. Can. Geotech. J. 50 (7), 723–734.